ELSEVIER

Journal of Nuclear Materials 241–243 (1997) 816–820

journal of nuclear materials

Studies on plasma edge transport and layer deposition by local injection of reactive gases during TEXTOR-94 discharges

U. Kögler *, F. Weschenfelder, J. Winter, H.G. Esser, V. Philipps, A. Pospieszczyk, B. Schweer, J. von Seggern, M.Z. Tokar', P. Wienhold

Forschungszentrum Jülich GmbH, Institut für Plasmaphysik, Association Euratom-KFA, 52425 Jülich, Germany

Abstract

To study local particle transport, silane was injected through a hole in a test limiter surface during discharges in TEXTOR-94. The gas injection lead to the deposition of a thin layer around the injection hole which was close to the area of the highest heat load. The layer was eroded in discharges without silane injection. The layer was not only formed by the injected silicon but also by a large amount of carbon which must originate from other plasma facing components. The preferential direction (symmetry line) of the deposition pattern is tilted by $\sim 25°$ relative to the magnetic field lines. Calculations with the ERO-TEXTOR code recover the general shape of the Si-deposition pattern. To get accordance between the calculations and the experimental results a strong electric field parallel to **B** and a sticking coefficient much smaller than 1 has to be considered to reproduce the low silicon deposition efficiency, whereas the tilting of the symmetry line can be explained by the existence of a radial electric field.

Keywords: TEXTOR-94; Limiter; 3D model; Monte Carlo simulation; Impurity transport; Erosion and particle deposition

1. Introduction

The control of material erosion on first wall elements such as a limiter or divertor is a serious problem in future fusion devices. High heat and particle fluxes may lead to erosion rates which are unacceptably high for long pulse operation. Since the net wall erosion is the result of several interdependent processes including surface and plasma edge physics a detailed understanding of individual processes and interaction mechanisms is necessary to actively control and mitigate erosion. The formation of a strong local impurity source of chemically eroded molecules or physically sputtered atoms can influence local and global plasma edge parameters, like the density and temperature of electrons, ions and neutrals, which, on the other hand, are the major quantities determining both the erosion and the prompt redeposition.

The concept of layer deposition by local injection of reactive gases was examined in TEXTOR as a possibility to actively control net erosion. It is based on the controlled injection of suitable reactive gases such as methane or silane close to or at the areas of highest erosion. It was clearly demonstrated that in the vicinity of an injection hole a film can be deposited even in areas where erosion occurs without gas injection [1,10]. Due to its similarity to methane which is chemically produced at graphite limiter surfaces, silane (SiD_4) is an ideal model system and its transport and deposition can be studied without interference from the major tokamak intrinsic impurities carbon or boron.

The ERO-TEXTOR code was developed to describe the experimental results. It is a local 3D-Monte Carlo code which, initially based on the ERO code [2,3], was enhanced including now the kinetic description of the one-particle distribution functions, curved limiter surfaces, a SOL defined by limiters, and ionization processes of eroded or injected molecules. It was found that local electric fields parallel to B and radial electric fields arising from gradients in the plasma parameters like electron temperature and density have a great influence on the shape of the

* Corresponding author. Tel.: +49-24 612 631; fax: +49-24 616 660; e-mail: u.koegler@kfa-juelich.de.

PII S0022-3115(96)00612-5

deposition pattern and also on the deposition efficiency. These fields are partly due to the conditions in the SOL and partly caused by the strong particle source.

2. Experimental

A variety of experiments with gas injection through a test limiter in TEXTOR-94 ($R = 1.75$ m, $r = 0.46$ m) was performed to see the influence of local impurity sources on the erosion of limiter material. The limiters were observed spectroscopically during the experiments. After the experiments the deposition patterns on the limiters were evaluated and surface analysis techniques were used to determine quantitatively the amount and the composition of deposited material. The limiter material, the injection rates and the plasma parameters were varied to see the influence on the different quantities.

Test limiters made of different materials (graphite EK98, steel, copper) were exposed to the TEXTOR-94 plasma. The plasma facing surface (100 mm × 60 mm) of the limiters had a double curvature with radii of 85 mm in toroidal direction and 60 mm in poloidal direction (see Fig. 1). For gas injection a hole was drilled through the limiter at a position 10 mm from the edge which is radially 10 mm behind the tangency point. During exposure the hole was located on the ion drift side of the limiter. This shows the higher heat load due to a longer connection length to the ALT-II limiter which defines the last closed flux surface (LCFS). For most of the experiments the limiter was inserted with its tangency point at the radial position of the LCFS with $r = 46.0$ cm or slightly outside the confined plasma at $r = 46.8$ cm. The location of the injection hole was also changed for some experiments (to the top of the limiter and from the ion to the electron drift side). Even if not discussed in this paper these results can also be well understood and reproduced with the model described below.

To determine the 2-dimensional distribution of the Si light emission the limiter was observed during the discharges from the top and from the side with a CCD camera equipped with Si I (251.7 nm) or Si II (634.7 nm) interference filters (see Fig. 1).

All results reported here were achieved during ohmically heated discharges with a plasma current $I_p = 355$ kA and a toroidal magnetic field $B_t = 2.25$ T. The line averaged density was feedback controlled to 3.0×10^{19} m^{-3}. This gives the following local plasma parameters: an electron temperature of $T_e \simeq 19$ eV and a density of $n_e \simeq 3.0 \times 10^{18}$ m^{-3} at the LCFS respectively. The electron density decays with an e-folding length of $\lambda_{ne} \approx 15$ mm and the electron temperature with an e-folding length of $\lambda_{Te} \approx 20$ mm.

Silane (SiD_4) gas was injected during the flat top phase (constant plasma current and density) of the tokamak discharges. The length of the gas puff was short (~ 1 s)

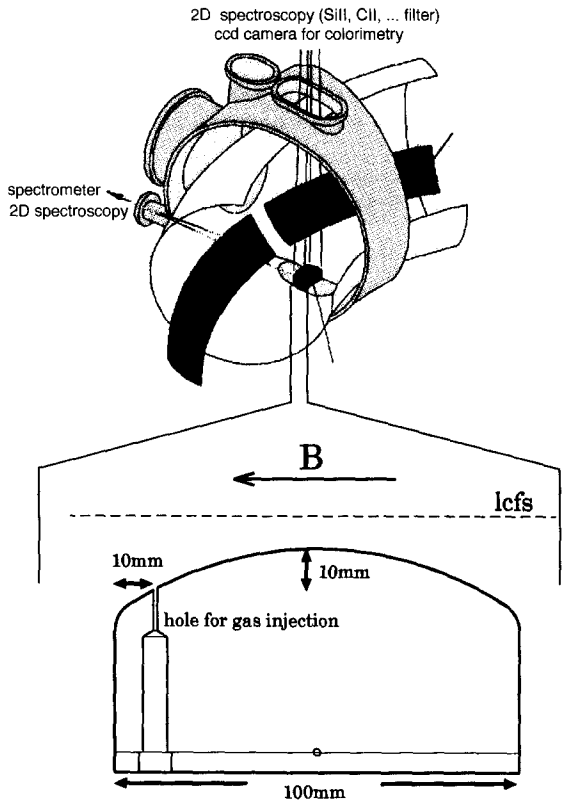

Fig. 1. Experimental setup of the limiter lock at TEXTOR-94 and the spectroscopic observation system. Geometry of the test limiter with the gas injection hole and the SOL geometry when the limiter is inserted at $a_{limiter} = 46.8$ cm.

compared to the length of the flat top phase of the discharges (~ 3–6 s). The gas puff started typically 1.0 s after reaching the flat top phase. This time with reproducible plasma conditions was used to look for changes in the spectroscopic observations caused by the gas puff in the previous discharge. The injection rate was varied between 4.3×10^{17} and 4×10^{19} SiD_4 molecules per discharge which corresponds to a flux of 8.6×10^{17} and 8×10^{19} molecules per second during the maximum of the gas puff. For higher injection rates the discharges with a line averaged electron density of 3.0×10^{19} m^{-3} disrupted, probably due to a thermal collapse.

3. Modelling

The ERO-TEXTOR-code is a Monte Carlo-implementation of a near-surface transport and film formation code. In a given volume and predefined geometry the code solves a Fokker–Planck equation for the evolution of an one-particle distribution function $f(x,t)$ of impurity ions in a relaxation time approximation. Drift and diffusion

terms are determined by the three relaxation times: the Spitzer times for dynamic friction, the deflection time and the energy exchange time [4,5]. The forces on a particle with charge Z_1 are an electric force caused by an electric field **E** and the Lorentz force with the vector product $[\mathbf{v} \times \mathbf{B}]$.

$$\vec{F} = \mathbf{Z}_1 e\left(\vec{E} + \left[\vec{v} \times \vec{B}\right]\right). \tag{1}$$

E is a sum of the following contributions:

$$\vec{E}(x) = \vec{E}_{\text{sheath}} + \vec{E}_{\text{pre-sheath}} + \vec{E}_{\text{radial}} + \vec{E}_{\parallel}. \tag{2}$$

The first two terms of the right hand side of Eq. (2) are due to the sheath and the magnetic pre-sheath and are normal to the material surface. The $\mathbf{E}_{\text{radial}}$ term is due to the local gradient of the electron temperature and gives rise to a gradient in the local electric potential of each flux tube. It is only present outside the LCFS and for a radial temperature gradient a radial electric field is resulting. These three terms have a component perpendicular to the magnetic field and induce an $\mathbf{E} \times \mathbf{B}$-force. The penetration depth of the sheath and presheath field is of the order of some hundred microns and the resulting perpendicular transport will only be a few millimeters or less. A bigger effect can be expected for the $\mathbf{E}_{\text{radial}}$ term since it is present all over the scrape-off-layer. Although weaker than the first two terms it gives rise to a perpendicular shift of the particle of several millimeters or more.

The last term is mainly due to the local electron source of injected neutral impurities (and the recycling deuterium ions). It has to be calculated from the local source strength and is determined by the force balance equation [6], which for the electrons is

$$\frac{\mathrm{d}}{\mathrm{d}l} n_e T_e = -e\mathbf{E}_{\parallel} n_e - 0.71 n_e \frac{\mathrm{d}T_e}{\mathrm{d}l}; \tag{3}$$

dl is to be taken along one flux tube (1D-model).

Equivalent force balance equations for the fuel and impurity ions must also be considered. Due to the relative increase of the local ion density at the point of ionization the electric field $\mathbf{E}_{\parallel}$ points away from this location and therefore changes direction when passing through the electron source: On the side directing towards the material surface it accelerates the ions towards the surface, whereas on the plasma facing side it gives rise to a loss of impurity ions into the plasma.

The plasma is prescribed to the code as a given background of the measured electron temperature and density profiles from atomic beam measurements. The impurity background flux is fixed as a given percentage of the electron density and the interaction of the plasma with the material surface is calculated for these local plasma parameters. The coupling with the 1D-model gives a first step to a selfconsistent treatment of the interaction of the background plasma with the impurity ions.

For the description of the dissociation/ionization behavior of the injected silane molecules a model experimentally evaluated in a low temperature plasma [7,8] is used. The electron temperature dependence is scaled to the rates for methane [9], with the exception that the SiD_4^+ is not stable and predissociates into SiD_2^+.

Since the sticking coefficients of the molecular radicals are not well known some assumptions have to be made: the neutral radicals SiD_x are almost not sticking to the surface with a reflection probability of 0.995 and are released thermally. The ionic radicals are accelerated in the sheath potential of $\sim 3.8\ kT_e$ (electron temperature on the limiter surface: $T_e \approx 8$–19 eV, depending on the radial position) to an energy of 25–72 eV, resulting in a lower reflection probability which was set to 0.7.

4. Results and discussion

The pattern of the deposited film was always localized around the injection hole with typical extensions of about 10–20 mm in toroidal and 5–20 mm in poloidal direction. The symmetry line of the pattern was in all cases (with the injection hole 40 mm away from the limiter tip) tilted away from the direction of the magnetic field lines by an angle of $\sim 25°$. This angle changes with the location of the injection hole, but is always tilted to the high-field side of the machine, as expected from an $\mathbf{E} \times \mathbf{B}$-drift with the **E** field pointing towards the limiter surface.

Fig. 2 shows a typical film pattern deposited on a stainless steel limiter after 10 discharges with gas injection of $(7.1 \pm 0.2) \times 10^{18}$ silane molecules per discharge and one discharge without gas injection as determined by the interference colors of the thin film [12]. The deposition

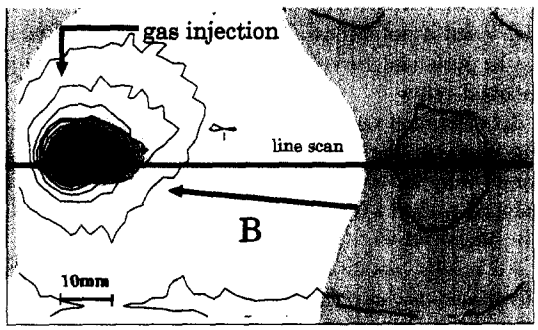

Fig. 2. Top view onto the deposited thin film determined by the interference colors of a stainless steel limiter after 10 discharges with gas injection and one discharge without gas injection (the color fringes of the film are calculated for optical constants of $n = 2.0$, $k = 0.005$ and for visible light with an angle of incidence of 45°). Contour lines from the modelling with the ERO-TEXTOR code of this discharge series.

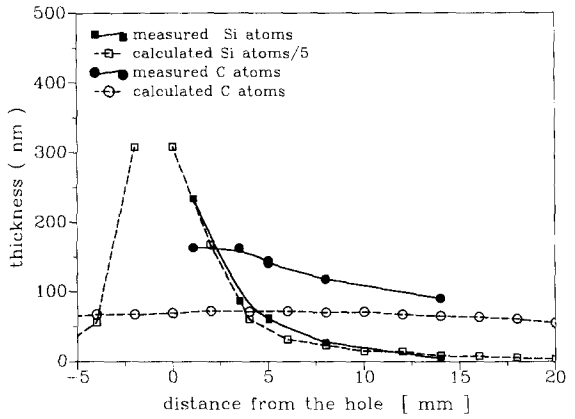

Fig. 3. Toroidal scan (see Fig. 2 for the geometry) of the composition of the deposited film (full lines from electron probe micro analysis (EPMA), dashed lines from modelling). Note that the calculated silicon thickness is divided by a factor of 5.

pattern is peaked at the injection hole where it reaches a thickness of about 500 nm and falls off toroidally with an e-folding length of $\lambda_{tor,film} \approx 8$ mm and poloidally with $\lambda_{pol,film} \approx 3$ mm. The contour lines in Fig. 2 show for comparison also the deposition pattern as modelled with the ERO-TEXTOR code for the measured plasma parameters. The major experimental findings can be reproduced. Both thickness patterns are peaking at the location of gas injection. The symmetry lines are tilted in the same direction and also the carbon deposition on the e-drift side caused by the plasma impurity background flow is well reproduced.

For the tilting of the deposition pattern away from the direction of the magnetic field lines a radial electric field of a strength of $\mathbf{E} = 1$–2 V/mm had to be considered. This is equivalent to $\mathbf{E} = -0.5\ \nabla_r \Phi_0$, were Φ_0 is the local sheath potential drop and ∇_r the radial gradient.

The post mortem analysis with an electron beam microprobe (Fig. 3) along a toroidal line through the gas injection hole, also shown in Fig. 2, reveals that about 50% of the film is codeposited carbon. This was also observed for a carbon limiter [1,11], but in the case of the stainless steel limiter this large amount of carbon can only originate from the background plasma. This is also suggested by the broad profile of the carbon deposition with its small dependence on the toroidal position. The modelling also shows this broad carbon deposition pattern, but the calculated fraction of codeposited carbon in the film is about 50% smaller in the area close to the injection hole. The very efficient way to codeposit carbon from the background plasma is due to a partial coverage of deposited carbon with silicon.

Integrating the deposited film thickness and assuming a mean film density of 5.4×10^{22} atoms per cm^3 (4.3×10^{22} atoms per cm^3 for the Si atoms and 6.5×10^{22} atoms per cm^3 for the C atoms [13]) and a silicon fraction of 50%, a deposition efficiency (deposited Si-atoms/injected Si-atoms) of less than 5% was found.

Such a low deposition efficiency can only be reproduced in the calculations if an additional transport parallel to the magnetic field lines is considered as it is described with the last term in Eq. (2). The strong local electron source of the injected silane molecules gives rise to a parallel electric field $\mathbf{E}_{\|}$. Without such a parallel electric field, but taking into account multiple dynamic sputtering and high reflection coefficients, a deposition efficiency greater than 65% is calculated. This number is nearly independent of small changes in the assumed plasma parameters (see Table 1). If the electric field $\mathbf{E}_{\|}$ is included, all particles ionized deeper in the plasma than the medium ionization length have a certain probability to be transported away from the limiter. Including such a loss channel for silane molecules to the SOL the deposition efficiency as modelled is lowered but still $\sim 35\%$. This indicates that even more complex mechanisms than those considered are involved, or that the database of cross sections is incomplete or erroneous.

Fig. 4a shows the tangential view of a CCD camera at the test limiter during a gas puff (Si I light, 251.7 nm). The picture was taken during the injection maximum corresponding to a rate of 5.4×10^{19} SiD_4 s^{-1}. The limiter was located 8 mm outside the LCFS (46.8 cm) during an ohmic discharge with a line averaged density of 3×10^{19} m^{-3}. The field of view is limited by a circular window, the limiter tip is placed at the lower part of the picture and its contour can be seen in the Si I light. The intensity maximum is located right above the injection hole but the light is spread all across the surface. Fig. 4b shows in comparison the Si I light intensity as calculated with the ERO-

Table 1
Deposition efficiency of the injected silane for different modelling scenarios. Plasma parameters are $n_e \approx 3 \times 10^{18}$ m^{-3} and $T_e \approx 19$ eV at the LCFS

Modelling parameter	Deposition efficiency (%)	
	without $\mathbf{E}_{\|}$	with $\mathbf{E}_{\|}$
Reflection coefficient of neutral and ionic species $R_{i,n} = 0$; no sputtering from background plasma	90	80
Reflection coefficient of neutral species $R_n = 0.995$ and of ionic radicals $R_i = 0.7$; no sputtering from background plasma	70	50
Reflection coefficient of neutral species $R_n = 0.995$ and of ionic radicals $R_i = 0.7$; multiple dynamic sputtering from background plasma	65	35

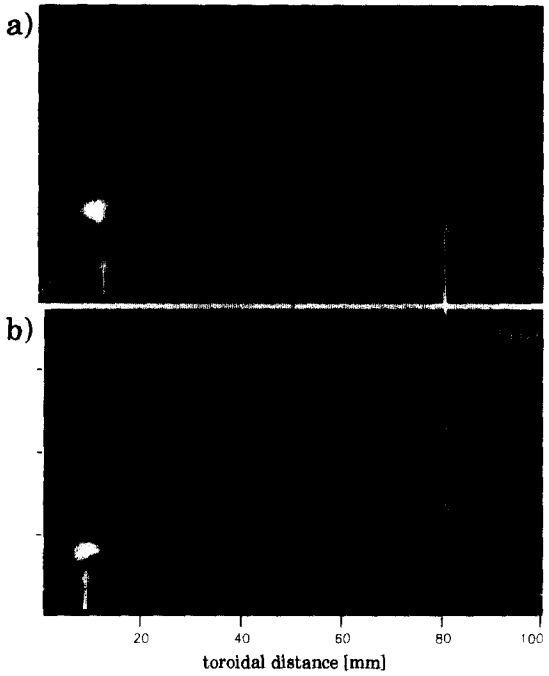

Fig. 4. Tangential view of the Si I emission ($\lambda = 251.7$ nm) at the test limiter during a gas puff at the maximum injection rate. (a) experimental observation; (b) simulation result.

TEXTOR code. The light is limited to the side of the limiter where the silane injection took place. This difference is likely to be due to the fact that the transport of the silicon across the surface by multiple deposition and reerosion may be underestimated and the sticking coefficient for ions is still to high. Also long range transport of silicon through the plasma which is then again recycled at the limiter is not included in the model. A particle leaving the volume which is taken into account for the calculations is no longer traced. An increase of the silicon background flux correlated to the injected amount of silane is not yet assumed.

5. Summary and conclusions

The method of layer deposition on wall components has been extensively studied on test limiters in the tokamak TEXTOR-94. With the injection of silane it could be shown that erosion dominated areas can be transformed into 'balanced' areas, where the erosion of the substrate can be reduced and an effective film deposition can be observed. The modelling with the ERO-TEXTOR code reflects the major features of the experiment, i.e. the deposition pattern and the spectroscopic information. Furthermore the modelling shows the importance of scrape-off-layer and local electric fields: The radial electric field $\mathbf{E}_{\text{radial}}$, caused by the gradient of the electron temperature gives rise to a poloidal transport of the injected molecules and therefore a tilting of the deposition pattern away from the direction of the magnetic field lines. The parallel electric field $\mathbf{E}_{\|}$, induced by the electron source of the silane injection itself, results in an effective transport of the injected species into the plasma and is therefore partly responsible for the very low deposition efficiency observed in the experiment. The numerical studies reveal that the cumulative occurrence of multiple sputtering, high reflection probabilities of the molecular fragments and the presence of the parallel electric field together give rise to a major loss effect of the injected molecules. Still a difference of about a factor ≥ 5 between the observed deposition efficiencies and the simulation results remain. Further investigation is necessary to illuminate other loss channels, which may be due to local changes in the electron density and temperature.

Acknowledgements

The authors like to thank P. Karduck, RWTH Aachen for the EPMA analysis of the limiter and M. Freisinger for data handling.

References

[1] H.G. Esser et al., J. Nucl. Mater. 220–222 (1995) 457.
[2] D. Naujoks et al., Nucl. Fusion 33 (1993) 581.
[3] D. Naujoks and R. Behrisch, J. Nucl. Mater. 220–222 (1995) 227.
[4] L. Spitzer, Physics of Fully Ionized Gases (Wiley, New York, 1962).
[5] D. Reiser, Eine Monte-Carlo-Methode zur Untersuchung von Verunreinigungsionen in Tokamak-Plasmen, JÜL-3173, Jülich.
[6] M. Tokar', Contrib. Plas. Phys. 36 (1996) 250.
[7] U. Fantz, thesis, Institut für Plasmaforschung, Universität Stuttgart (1995).
[8] G. Schneider, diplomarbeit, Institut für Plasmaforschung, Universität Stuttgart (1994).
[9] A.B. Erhardt and W.D. Langer, Report PPPL-2477 (Princeton, NJ, 1987).
[10] U. Kögler, J. Winter, H.G. Esser et al., Proc. 22nd EPS-Conf. on Controlled Fusion and Plasma Physics, IV-281, Bournemouth.
[11] G. Mank, J.A. Boebo et al., these Proceedings, p. 821.
[12] P. Wienhold, F. Weschenfelder and J. Winter, Nucl. Instr. Meth. Phys. Res. B94 (1994) 503.
[13] J. von Seggern, J. Winter et al., J. Nucl. Mater. 220–222 (1995) 677.